INTERNATIONAL JOURNAL FOR NUMERICAL METHODS IN FLUIDS
Int. J. Numer. Meth. Fluids **31**: 1321–1331 (1999)

A NUMERICAL MODEL FOR RUN-UP OF BREAKING WAVES

H. JOHNSGARD*

Department of Mathematics, University of Oslo, Oberst Rodes veu 446, 1152, PO Box 1053 Blindern, Oslo, Norway

SUMMARY

In the present paper, the numerical method for the three-dimensional run-up, given in Johnsgard and Pedersen ['A numerical model for three-dimensional run-up', *Int. J. Numer. Methods Fluids*, **24**, 913–931 (1997)], is extended to include wave breaking. In the fundamental problem of run-up of a uniform bore, the present model is compared with analytical solutions from the literature. The numerical solutions converge, but very slowly. This is not due to the numerical model, but rather to the structure of the solutions themselves. Numerical results for two realistic but simplified tsunami cases are also presented. In the first case, two-dimensional simulations are performed concerning the run-up of a tsunami in Portugal, in the second case, the three dimensional wave pattern generated after a slide in Tafjord, Norway in 1931, is studied. A discussion of different aspects of the model is summarized at the end of the paper. Copyright © 1999 John Wiley & Sons, Ltd.

KEY WORDS: run-up; wave breaking; tsunami

1. INTRODUCTION

The study of wave breaking during run-up is important for two reasons. First, it occurs in many practical situations, and influences both run-up heights and the destructive potential of the waves. Second, wave breaking may be hidden in numerical solutions for shallow water equations. Hopefully the readers of this paper will gain an improved understanding of when such breaking may occur, and how to identify it.

A full description of wave breaking is very complicated, and the kind of turbulence modelling that is needed is still not available. A common approach, which is valid in the long-wave limit, is to describe the bore that is formed during breaking as a discontinuity. The key feature is that no mass and momentum are lost during breaking, and methods used for acoustic shock waves may be adapted. Such techniques may be based on a patching of fluxes for mass and momentum at the bore discontinuity. A more sophisticated use of analytical expressions is made in the Gudonov method, where the surface profile is approximated by a piecewise constant function and the solution on an advancing time step is found after solving a series of Riemann problems. A lot of techniques have been developed from this basis. A simpler approach is to include some kind of artificial diffusion, either implicitly inherited in the numerical scheme, or stated explicitly. For refined grids and vanishing diffusion all these methods converge towards the same limit, as long as mass and momentum are conserved.

* Correspondence to: Department of Mathematics, University of Oslo, Oberst Rodes veu 446, 1152, PO Box 1053 Blindern, Oslo, Norway.

CCC 0271–2091/99/241321–11$17.50

Received February 1998
Revised December 1998

In the present paper, the method developed by Johnsgard and Pedersen [1] is generalized to include wave breaking. The focus is not on the shock treatment itself, but rather on the processes involved when shocks are interacting with moving shorelines. Hence, the simplest possible treatment of the bore has been selected: an artificial diffusion stated directly in the momentum equation. It is observed that the slow convergence reported in this paper is not due to this particular selection of shock treatment.

Hibberd and Peregrine [2], made a study of bore run-up related to the present one. Two new features are present here: the Lagrangian description, which makes the run-up calculations more accurate, and the capacity of solving three-dimensional problems.

Classical analytical theory, discussed in Section 3, shows an extremely fast bore development near the free tip, and the outcome of this process substantially influences the run-up heights. This gives rise to two fundamental problems. First, extremely dense grids are needed to get converged results. Second, since real world bores have a finite length, the bore development near the shore may not be physically relevant. A discussion of these questions, also including a bottom drag, will be given subsequently.

The numerical simulation of two simplified but realistic tsunami cases has also been included. The topography has been selected simple enough to make it possible to identify the different physical processes that are involved, and to see how they are handled.

2. THE MODEL

Gravity waves in inviscid and incompressible fluids are considered. Lengths of the waves and scales for bottom variations are sufficiently large for a hydrostatic pressure distribution to apply. The governing equations are the Airy equations, which form a fully non-linear, non-dispersive wave model (see, for instance, Reference [3]). Lagrangian co-ordinates are introduced to enable a tracking of moving shorelines. A simple model of slide events is included into the model through a time-dependent bottom topography.

2.1. Governing equations

Following Reference [1], Lagrangian enumeration co-ordinates a and b are introduced, marking vertical columns of water. Since the label co-ordinate system may be curvilinear, the computational domain in the a, b plane will be a fixed rectangle. The continuity equation is

$$H\frac{\partial(x, y)}{\partial(a, b)} = V(a, b), \tag{1}$$

where $H \equiv h + \eta$ is the total water depth and

$$V = H(a, b, 0)\left.\frac{\partial(x, y)}{\partial(a, b)}\right|_{t=0}$$

has the interpretation of volume density per area in the (a, b) plane. The x component of the momentum equation may be written as

$$\frac{\partial^2 x}{\partial t^2} = -\frac{H}{V}\frac{\partial(\eta, y)}{\partial(a, b)} + \frac{\gamma}{H_0}\frac{\partial}{\partial a}\left(\frac{H^{q+1}}{H_0}\frac{\partial u}{\partial a}\right) + \frac{\gamma}{H_0}\frac{\partial}{\partial b}\left(\frac{H^{q+1}}{H_0}\frac{\partial u}{\partial b}\right) - \frac{C_D|\vec{v}|u}{H_n}, \tag{2}$$

where $H_n = \max(H, n)$. Selecting $n > 0$, the unphysical singularity in the expression for bottom drag is removed. The y component takes on a similar form.

Introducing horizontal and vertical length scales, l_h and l_v respectively, it is found that the governing equations may be written in non-dimensional form simply by replacing g with 1 and C_D and γ with $\hat{C}_D = (l_h/l_v)C_D$ and $\hat{\gamma} = (l_h/l_v)\gamma$ respectively.

2.2. Numerical equations

A discrete approximation to a function f, at $a = i\Delta a$, $b = j\Delta b$ and $t = p\Delta t$, is denoted by $f = f_{i,j}^{(p)}$. The governing equation is discretized in an Arakawa B grid, where the primary unknowns are

$$\eta_{i,j}^{(p)},\ H_{i,j}^{(p)},\ x_{i+1/2,j+1/2}^{(p)},\ y_{i+1/2,j+1/2}^{(p)},\ u_{i+1/2,j+1/2}^{(p+1/2)},\ v_{i+1/2,j+1/2}^{(p+1/2)}.$$

The discrete equations take the same form as in [1], except for the inclusion of new terms in the momentum equations. The new terms are included by a split step procedure. Only the x component is described. The first step is identical to the discretization in [1],

$$\left[\frac{(u^{(+)} - u^{(p-1/2)})}{\Delta t} = -\left[g\frac{\overline{\bar{H}}^{ab}}{\bar{V}_0^{ab}}(\overline{\delta_a\eta\delta_b y}^{b} - \overline{\delta_b\eta\delta_a y}^{a})\right]^{(p)}\right]_{i+1/2,j+1/2}. \tag{3}$$

In the next three steps, the diffusion term and the bottom friction are included,

$$\left[\frac{u^{(++)} - u^{(+)}}{\Delta t} = \left[\frac{\Delta t\beta}{\bar{H}_0}\delta_a\left(\frac{H^{q+1}}{H_0}\delta_a u^{(++)}\right)\right]^{(p)}\right]_{i+1/2,j+1/2}, \tag{4}$$

$$\left[\frac{u^{(+++)} - u^{(++)}}{\Delta t} = \left[\frac{\Delta t\beta}{\bar{H}_0}\delta_b\left(\frac{H^{q+1}}{H_0}\delta_b u^{(+++)}\right)\right]^{(p)}\right]_{i+1/2,j+1/2}, \tag{5}$$

$$\left[\frac{u^{(p+1/2)} - u^{(+++)}}{\Delta t} = -\frac{C_D|\vec{v}^{(p-1/2)}|u^{(p+1/2)}}{H_n^{(p)}}{}^{(p)}\right]_{i+1/2,j+1/2}. \tag{6}$$

Here δ_a and $\bar{f}^{(a)}$ denote a central difference and average operators, and $\gamma = \beta\Delta t$. The y component is treated similarly. New displacements are then computed by

$$[\delta_t x = u, \quad \delta_t y = v]_{i+1/2,j+1/2}^{(p+1/2)}. \tag{7}$$

It is noticed that the strength of the diffusion term is reduced as the grid is refined, while the number of grid points within a bore will be held at a fixed level. If β is to large, the bore becomes to wide, if β is to small, the numerical solution becomes contaminated by grid noise. Care has been taken so that a good value has been selected for each case.

The introduction of a diffusion term will tend to increase the stability of the numerical solutions. For instance, the non-linear production of grid noise (aliasing), reported by [1], will be reduced. Actually, an introduction of artificial diffusion is one of the classical approaches for controlling aliasing. In other cases, the physical relevancy of the increased stability may be questionable. For instance, the present model is not able to reproduce a plunging breaking at all.

3. RUN-UP OF A BORE ON A UNIFORM SLOPE

In the absence of artificial diffusion and bottom friction, the model has been extensively tested in [1]. There is a need to include a test where numerical and analytical solutions concerning bore interacting with shorelines is compared. A suitable analytical theory is then the one concerning run-up of uniform bores on uniform slopes. This theory, which was developed in

the early 1960s, is based on the present governing equations, although without bottom drag. A short review of this theory will be given, then the paper returns to the presentation and discussion of the numerical solution.

3.1. Bore run-up, existing theory

The bore run-up may be divided into several phases:

1. On the *surf period*, the bore propagates from the edge of the sloping region to the initial shoreline. A differential equation for the bore velocity as function of the layer thickness in front of the shock was found by Keller *et al.* [4], by combinations of characteristic expressions behind the bore and bore conditions. The main feature of the solution of this equation is that the bore vanishes as it approaches the shoreline, while the bore strength relative to the layer thickness in front of the shock goes to infinity. There is an almost explosively fast bore development near the shore. For instance, for an initially bore height of 0.25 times the depth in front of the bore, it is found that the particle velocity behind the bore increases from 1.325 to 1.659 during the last 1/5000 fraction of the slope. A good numerical representation of this phenomenon requires an extremely dense grid. As shall be seen, the run-up heights depend crucially upon the outcome of this process. Of course, the physical relevancy is highly questionable.
2. The next phase is the *bore run-up*. Analytical results for this process are given by Shen and Meyer [5]. They transformed the governing equations to a linear set by using canonical variables, and showed that the shoreline particle is insensitive to other wave motions. Its position is a quadratic function of time, and the run-up height is given by $R = u_0^2/g$, where u_0 is the velocity behind the bore as the bore arrives the shoreline. The layer thickness near the free tip is extremely thin, given by $H = (x - x_s)^2/9gt^2$, where t denotes the time after the bore has arrived at the shoreline. These results are given in unscaled form.
3. The theory developed by Shen and Meyer [5] also predicts the generation of a landward-facing bore during *backwash*. An almost stationary bore is formed. The effect of this bore is to bring the rapid fluid particles during backwash nearly to rest, and the bore vanishes when the free tip has reached the bore. The water level near the shore will be twice the height of the incident bore, the reflected wave that now has been formed will break, and a seaward-facing bore, propagating seawards, with low, gentle waves behind it, will eventually be formed.

3.2. Model set-up

The selected bottom profile is a linear slope in the near-shore region connected to a deep, flat bottom. The equations are put into non-dimensional form by selecting the slope length and the depth in the flat region before the bore arrives as horizontal and vertical length scale respectively. A uniform bore with height 0.25 and initial position 1.1 is now incident on the slope, see Figure 1(a). As in [1], a variable initial grid is employed, where the grid size is proportional to $\sqrt{h}$.

Figure 1 shows that the phases of the bore run-up predicted by the analytical theory is reproduced, at least qualitatively. Figure 2 (a) shows the shoreline elevation for different grids, and the corresponding analytical solution by Meyer. The slow convergence is due to the heavy costs of resolving the inner part of the slope, where the bore develops fast, and are not due to the particular shock treatment. The fluid layer near the free tip is extremely thin. Hence, if we redefine the inundation length to be the position where the layer thickness is, say, 10% of the initial shock height, we find much better convergence (Figure 2(b)).

An improved physical description of the thin fluid film is achieved by introducing bottom drag into the model. Figure 2(c) and (d) shows results for two different values for $\hat{C}_D$. The correct value of $\hat{C}_D$ depends on the ratio between the horizontal and vertical scales, for $C_D = 0.001$, the two cases correspond to $l_h/l_v = 10$ and $l_h/l_v = 100$ respectively. Note that, for the first case, you have improved convergence. For the second case, you have an even faster convergence, and towards a lower limit.

It is noted that $n = 0$ for the runs presented in this section. The singularity in the expression for bottom drag did not lead to unreasonable results. This is not always the case, as will be demonstrated subsequently.

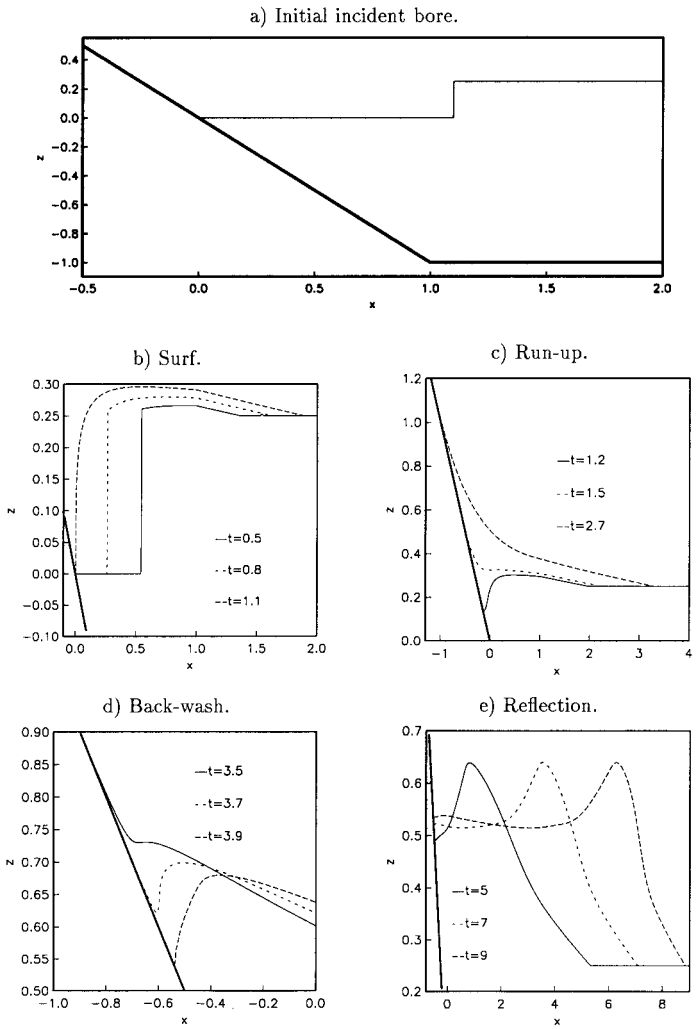

Figure 1. Surface profiles for bore run-up. Average initial grid size is Δa.

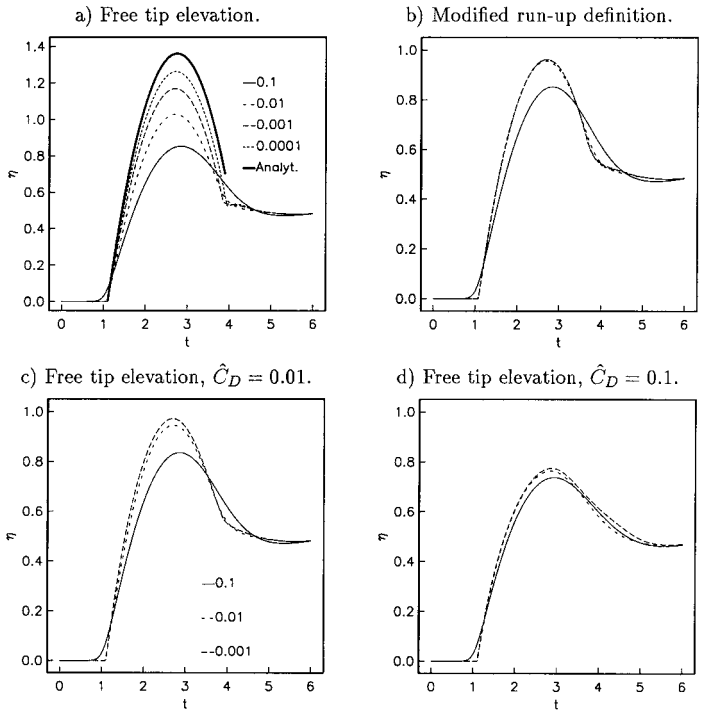

Figure 2. Grid refinement tests. Curve legends denote the average initial grid size. Right panels: curve legends given in left panels.

4. RUN-UP OF THE 1969 GORRINGE BANK TSUNAMI

In this section we study the run-up and breaking of a tsunami at the coast of Portugal. The initial profile is extracted from a two-dimensional numerical solution of the Boussinesq equation, reported by Gjevik *et al.* [6], at an instant where the main pulse reaches a depth shallow enough for the omission of dispersive effects. The actual bottom topography is simplified substantially to consist of a linear slope, 5 km wide, connected to a flat bottom of 20 m depth. The bottom topography and initial wave profile is shown in Figure 3 (upper panel). To enable a discussion of some principal aspects of this situation, runs for a more shallow case, with a maximum depth of 10 m, have also been performed. The bottom drag is specified according to $C_D = 0.003$ and $n = 0.5$ m. Runs for $C_D = 0$ and $n = 0$ are also reported.

4.1. Results

Converged numerical results showing the development of the surface profile during surf and run-up are demonstrated in Figure 3. It is observed from the mid-panel that no net amplification takes place over the slope. The convergence for the shoreline particle is demonstrated in Figure 4(a). Figure 4(b) demonstrates that no convergence seems to occur during backwash when the singularity in the expression for bottom stress is not removed. Of course, the singularity is not physical, and one may anticipate that an improved physical description of the thin film of fluid leads to better convergence.

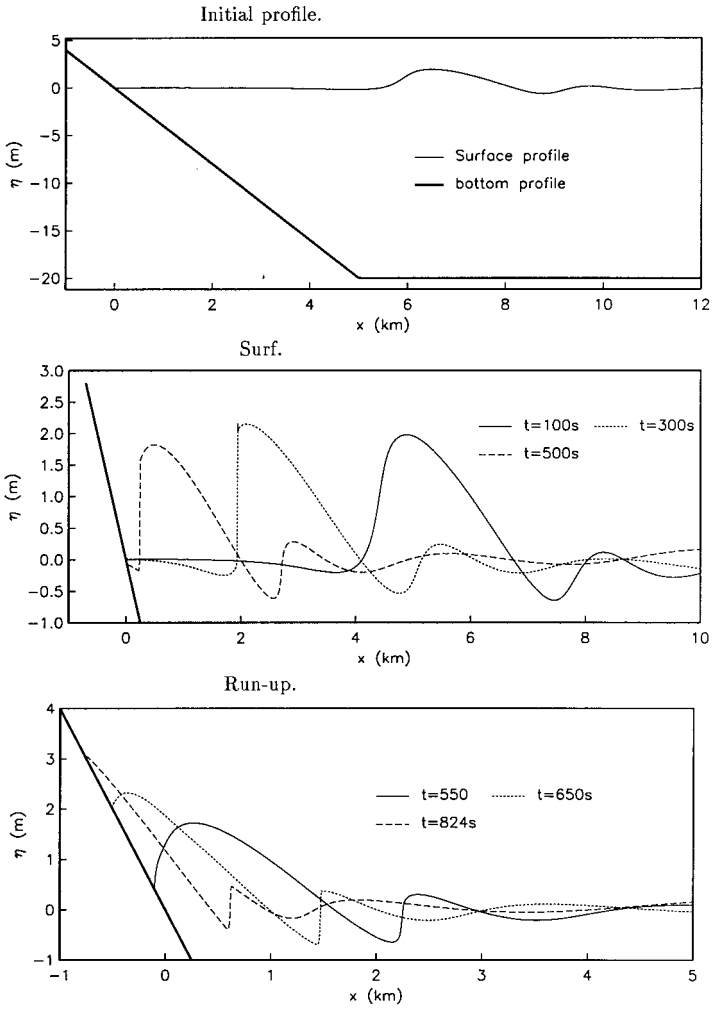

Figure 3. Surface profiles for Portuguese tsunami event. Average inital grid size is 5 m.

Figure 4(c) and (d) show similar results for the shallow case (maximum depth 10 m). It is observed that the curves have similar shapes as for the standard case, while the waves have now been substantially damped during shoaling.

Figure 4(e) shows that the bottom stress is vital to avoid slow convergence. As for the previous case, the convergence may be speeded up by redefining the inundation length; Figure 4(f) tracks the position where the layer thickness is 0.25 m.

5. A SIMPLE MODEL OF THE TAFJORD EVENT

A numerical study of the slide and tsunami event at Tafjord was given by Harbitz *et al.* [7], with a linear and non-dispersive model. Probably both non-linearity and dispersion should be considered. Here, the effects of non-linearity and wave breaking are studied for a simplified fjord geometry, where the scales and slide geometry roughly match the Tafjord case.

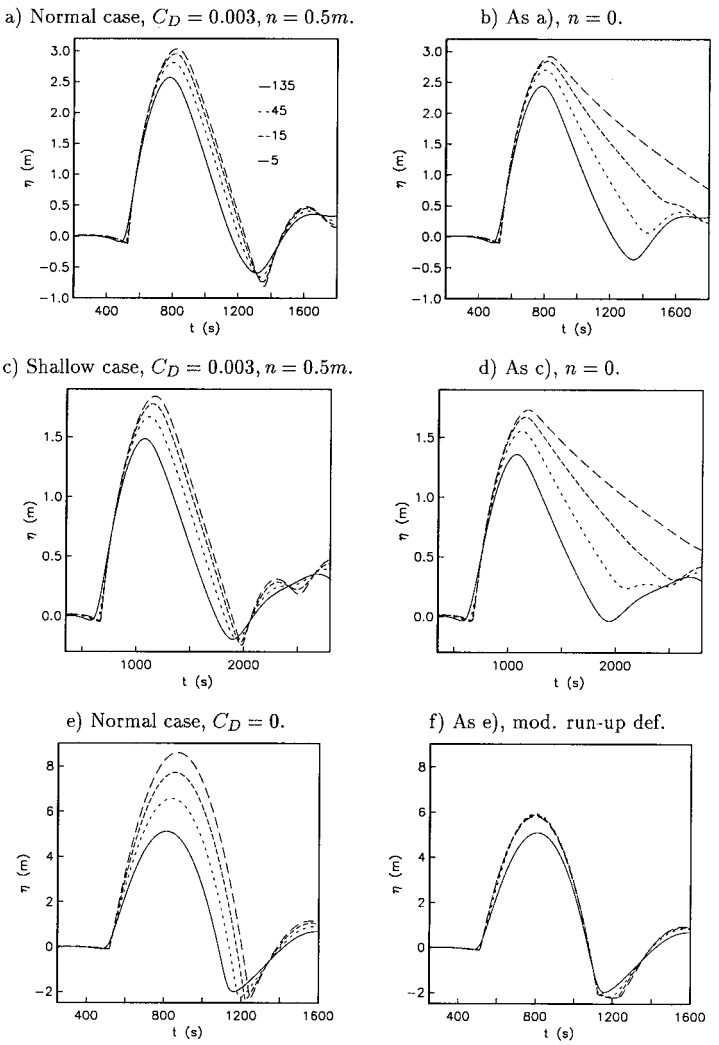

Figure 4. Free tip elevations, grid refinement tests. Curve legends given in (a) denote the average initial grid size in meters.

The bottom topography is assumed to be parabolic across and uniform along the fjord. The slide is $2B_s$ wide, the frontal length is L_s and the slide is uniform behind the front. The slide height is denoted by A.

The x-axis is aligned across the fjord and the y-axis is aligned along the beach where the slide is impinging. The slide centre starts at $(x_0, 0)$ and travels a distance R in a time T_R, along a line perpendicular to the initial shoreline. The bottom topography is then given by

$$h(x, y, t) = h_{\max} 4x(L - x)/L^2 - \hat{h}(x - x_r(t), y),$$

where $\hat{h}$ defines the shape of the slide and $x_r(t) = x_0 + R(\sin(t\pi/2T_R))$ is the position of the centre of the slide. For $t > T_R$, the slide remains at rest. The slide body is described by the function

$$\hat{h}(s,p) = A\cos^2\left(\frac{s\pi}{2L_s}\right)\cos^2\left(\frac{p\pi}{2B_s}\right),$$

for $0 < s < L_s$, $-B_s < p < B_s$,

$$\hat{h}(s,p) = A\cos^2\left(\frac{p\pi}{2B_s}\right),$$

for $s < 0$, $-B_s < p < B_s$, and $\hat{h} = 0$ elsewhere.

In the present case, $A = 75$ m, $L = 1200$ m, $h_{\max} = 180$ m, $L_s = B_s = 133$ m, $x_0 = -133$ m, $R = 528$ m, $T_R = 16.6$ s and $C_D = 0.003$ all have been selected.

5.1. Results

The generation of waves due to the slide is demonstrated in Figure 5. It is noticed that a roughly semi-circular bore propagates away from the slide area and runs up on the opposite

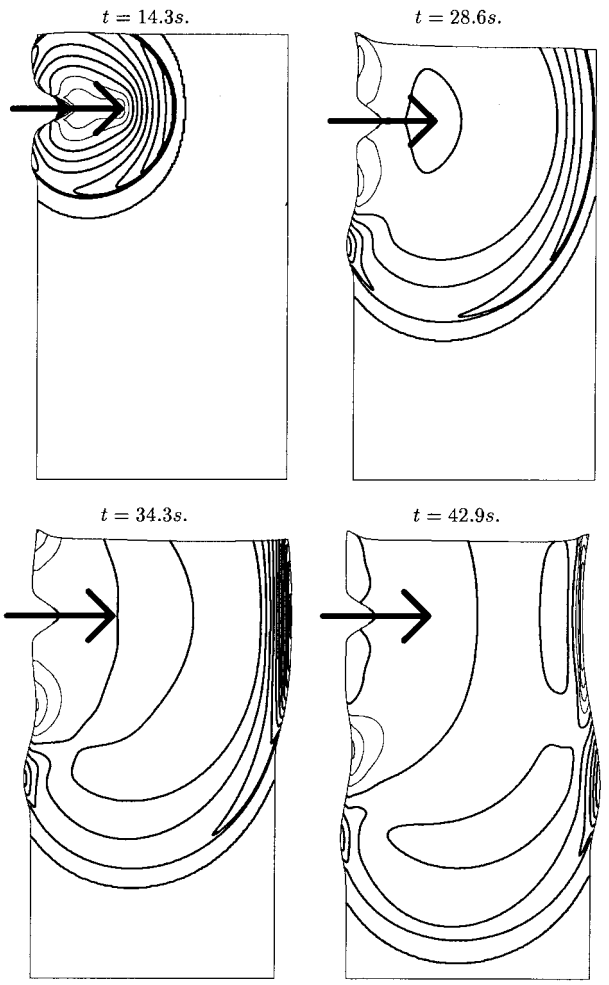

Figure 5. Time evolution of slide generated waves at Tafjord, 400 grid points across the fjord. Contour increments 5 m, thick lines for elevation.

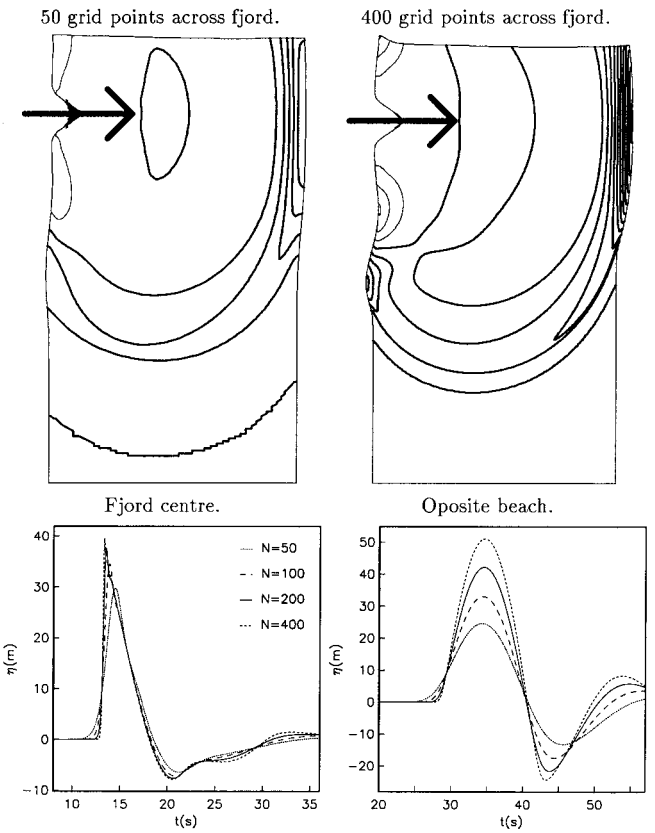

Figure 6. Grid refinement tests concerning the Tafjord case. Upper panels: $t = 34.3$ s, contour increments 5 m, thick lines for elevation. Lower panels: time profiles of the surface elevation at fjord centre and opposite beach, curve legends given in left panel, N denotes number of grid points across the fjord.

beach. Figure 6 shows grid refinement tests. Notice that the breaking is almost impossible to identify for the coarse grid. For the finest grid, the results seem to have converged, except near the shoreline, which is consistent with the results from the previous two-dimensional cases. Also, notice that the model seems to handle the situation with an obliquely incident bore on a shore. Finally, runs for $C_D = 0$ showed that this parameter had no substantial impact on the present result. However, for an even denser grid, it is expected that this parameter will be important near the shore. The parameter would be more important for a more shallow basin.

6. SUMMARY

A numerical model for the three-dimensional run-up of long waves has been generalized to include wave breaking. Comparison with analytical solutions showed convergence during grid refinement. The convergence was very slow due to the high grid density needed to resolve the details in the rapid bore development near the shoreline. The slow convergence is confined to a region near the free tip, where the fluid layer is very thin during run-up and backwash. An introduction of a bottom drag term, improving the physical description of the movement in this layer, speeded up the convergence substantially. This phenomenon was most pronounced

for very shallow cases, where bottom drag is of overall importance. It was necessary to remove the singularity in the expression for bottom drag to achieve fast convergence, even for deep backwash.

Many types of numerical diffusion, smoothening and filtering influence wave breaking in a similar manner as the present method. For coarse grids, the bores that are developed will, in general, be wide, and it is likely that the breaking may not be recognized. Figure 6 (upper left panel) demonstrates this feature. Grid refinements, linked to a reduction in numerical diffusion, will clear the picture, as in the right panel.

ACKNOWLEDGMENTS

The present research has been partially financed by the Commission of the European Communities under the contract ENV4-U96-0297, as part of the international project GITEC-TWO. The author is also grateful to Professor Geir Pedersen for interesting and fruitful discussions.

REFERENCES

1. H. Johnsgard and G. Pedersen, 'A numerical model for three dimensional run-up', *Int. J. Numer. Methods Fluids*, **24**, 913–931 (1997).
2. S. Hibberd and D.H. Peregrine, 'Surf and run-up on a bore: a uniform bore', *J. Fluid Mech.*, **95**, 323–345 (1979).
3. D.H. Peregrine, 'Equations for water waves and the approximations behind them', in R.E. Meyer (ed.), *Waves on Beaches*, Academic Press, New York, 1972, pp. 357–412.
4. H.B. Keller, D.A. Levine and G.B. Whitham, 'Motion of a bore over a sloping beach', *J. Fluid Mech.*, **7**, 302–316 (1960).
5. M.C. Shen and R.E. Meyer, 'Climb of a bore on a beach, 3: run-up', *J. Fluid Mech.*, **16**, 113–125 (1963).
6. B. Gjevik, G. Pedersen, E. Dybesland, C.B. Harbitz, P.M.A. Miranda, M.A. Baptista, L. Mendes-Victor, P. Heinrich, R. Roche and M. Guesmia, 'Modeling tsunami from earthquake sources near Gorringe Bank southwest of Portugal', *J. Geophys. Res.*, **102**, 27931–27949 (1997).
7. C.B. Harbitz, G. Pedersen and B. Gjevik, 'Numerical simulation of large water waves due to landslides', *J. Hydraul. Eng.*, **119**, 1325–1342 (1993).

